Unilateral Mitochondrial-Hemodynamic Coupling and Bilateral Connectivity in the Younger and Older Prefrontal Cortex of Healthy Adults

Claire Sissons , Fiza Saeed , Caroline Carter , Kathy Lee , Kristen Kerr , Sadra Shahdadian , Hanli Liu *

Posted Date: 29 August 2023

doi: 10.20944/preprints202308.1869.v1

Keywords: Age difference in prefrontal cortex; mitochondrial and hemodynamic coupling; prefrontal cortical connectivity; resting state functional connectivity; broadband near-infrared spectroscopy

Article

Unilateral Mitochondrial-Hemodynamic Coupling and Bilateral Connectivity in the Younger and Older Prefrontal Cortex of Healthy Adults

Claire Sissons [1], Fiza Saeed [1], Caroline Carter [1], Kathy Lee [2], Kristen Kerr [2], Sadra Shahdadian [1] and Hanli Liu [1,*]

[1] Department of Bioengineering, University of Texas at Arlington, Arlington, TX, 76019, USA
[2] School of Social Work; University of Texas at Arlington, Arlington, TX, 76019, USA
* Correspondence: hanli@uta.edu.

Abstract: A recent study demonstrated that noninvasive measurements of cortical hemodynamics and metabolism in the resting human prefrontal cortex can facilitate quantitative metrics of unilateral mitochondrial-hemodynamic coupling and bilateral connectivity in infraslow oscillation (ISO) frequencies in young adults (YA). The ISO includes three distinct vasomotions with endogenic (E), neurogenic (N), and myogenic (M) frequency bands. The goal of this study was to prove the hypothesis that there are significant differences between young and older adults (OA) in the unilateral coupling (uCOP) and bilateral connectivity (bCON) in the prefrontal cortex. Accordingly, we performed measurements from 24 OA (67.2 ± 5.9 years of age) using the same 2-channel broadband near-infrared spectroscopy (bbNIRS) setup and resting-state experimental protocol as those in the recent study (*Shahdadian et al, Cerebral Cortex Communications*, 2022). After quantification of uCOP and bCON in three E/N/M frequencies and statistical analysis, we demonstrated that OA had significantly weaker bilateral hemodynamic connectivity but significantly stronger bilateral metabolic connectivity than YA in the M band. Furthermore, OA exhibited significantly stronger unilateral coupling on both prefrontal sides in all E/N/M bands, particularly with a very large effect size in the M band (> 1.9). These age-related results clearly support our hypothesis and were well interpreted following neurophysiological principles. The key finding of this paper is that the neurophysiological metrics of uCOP and bCON are highly associated with age and may have the potential to become meaningful features for human brain health and be translatable for future clinical applications, such as early detection of Alzheimer's disease.

Keywords: age difference in prefrontal cortex; mitochondrial and hemodynamic coupling; prefrontal cortical connectivity; resting state functional connectivity; broadband near-infrared spectroscopy

1. Introduction

The enigmatic puzzle of brain function in young and older adults has intrigued scientists for years, including the prefrontal cortex, which is closely associated with human cognition as evidenced by many studies [1-5]. As aging progresses, a complex interplay of neurophysiological changes, such as mitochondrial and vascular alterations, shapes the performance of the human brain in young adults (YA) and older adults (OA), unveiling cognitive decline and its impact on executive mechanisms [6,7]. Recently our research team developed a new noninvasive measurement and quantification method that permits objective estimates of unilateral mitochondrial-hemodynamic coupling and their bilateral connectivity in the human frontal cortex [8]. This study focused on the impact of aging on the unilateral coupling and bilateral connectivity of mitochondrial and vascular/hemodynamic alterations in the resting prefrontal cortex in two distinct age groups. We aimed to shed light on how aging influences local and bilateral coherence and thus connectivity of neurophysiological activity in the prefrontal regions. Understanding the age-related shifts in neurophysiological mechanisms is crucial because they may impact various aspects of daily life, including decision-making, problem-solving, and attentional control [9].

Preprints (www.preprints.org) | NOT PEER-REVIEWED | Posted: 29 August 2023 doi:10.20944/preprints202308.1869.v1

1.1. Unilateral Metabolic-Hemodynamic Coupling and Bilateral Connectivity

Because of its high-level neuronal activity and cerebral metabolism, the human brain generally consumes a large amount of oxygen and glucose, which is continuously supported by an abundant oxygenated blood supply [8]. Cytochrome c oxidase (CCO) is a mitochondrial enzyme that consumes oxygen to produce adenosine triphosphate (ATP). The continuous and active synthesis of ATP by CCO provides intracellular energy to neurons and is essential for the normal operation of the human brain [10,11]. Thus, a close correlation or coherence must exist between local mitochondrial (or metabolic) and neurovascular (or hemodynamic) coupling, which is termed metabolic-hemodynamic coupling hereafter. Specifically, this study investigated unilateral coupling (uCOP) on each side of the human prefrontal cortex, namely, $uCOP_{left}$ and $uCOP_{right}$. These two quantifies reflect the balance between local neuronal metabolism (i.e., redox state of CCO) and oxygenated hemodynamics (i.e., oxygenated hemoglobin concentration, HbO) on each lateral side of prefrontal cortex [8]. In the meantime, we also calculated bilateral coherence of HbO (or CCO) signals of the prefrontal cortex, which is termed bilateral hemodynamic (or metabolic) connectivity, $bCON_{HbO}$ ($bCON_{CCO}$) of the resting prefrontal cortex. A larger coherence value indicates a stronger bilateral connectivity bilaterally [12].

1.2. Three Infraslow Oscillation Bands in Cerebral CCO and HbO Signals

Vasomotion is a key contributor to metabolic and hemodynamic oscillations and has been explored in studies focusing on cerebral metabolic activity [6,7]. The relaxation and contraction patterns of the blood vessel walls have been identified as the driving forces behind the infraslow oscillations (ISO) observed in cerebral hemodynamic signals [13,14] [15,16]. Researchers have discovered three intrinsic rhythm bands within cerebral hemodynamic signals that align with the specific physiological and/or biochemical activities of the vascular wall layers [8,11,17]. The three frequency bands were classified as endogenic (E) (0.005-0.02 Hz), neurogenic (N) (0.02-0.04 Hz), and myogenic (M) (0.04-0.2 Hz) rhythms, as shown in Figure 1(a) [8,18,19]. The E band corresponds to cycles of dilation and contraction in the endothelial layer, influenced by the release of vasoactive factors, such as nitric oxide (NO), free radicals, prostacyclin, endothelium-derived hyperpolarizing factor, and endothelin [20,21]. The N band involves the modulation of vessel dilation and contraction cycles by the oscillation of vasoactive ions and neurotransmitters released from neurons. Lastly, rhythmic M activity is a result of the relaxation and contraction of smooth muscle cells within the vascular walls. Figures 1(a) illustrates the anatomical structures and respective rhythm frequencies of the three ISO components at a local cerebral site [22]. Figures 1(b) and 1(c) further graphically explain the bilateral prefrontal connectivity and unilateral coupling derived from the HbO and CCO signals, respectively. The mathematical principle and operation to derive the three E/N/M bands are shown schematically in Section A of the Supplementary Materials.

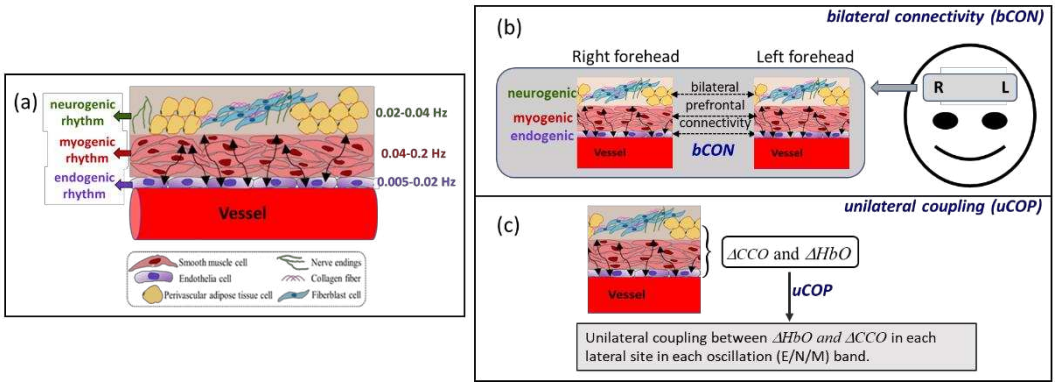

Figure 1. (a) Schematic illustration of a piece of blood vessel surrounded with three anatomical components [10,22] that facilitate spontaneous infraslow oscillations with endogenic (0.005-0.02 Hz), neurogenic (0.02-0.04 Hz), and myogenic rhythms (0.04-0.2 Hz). (b) Schematic illustration of bilateral prefrontal connectivity of hemodynamic or vascular oscillation in each of three ISO frequencies. (c)

 doi:10.20944/preprints202308.1869.v1

Schematic illustration of unilateral prefrontal coupling between hemodynamic and metabolic oscillations in each of three ISO frequencies.

Over time, the blood vessel walls become weaker or stiffer, causing a reduction in hemodynamic rhythms in the human brain. For example, vasomotion malfunction has been observed in OA and in patients with different diseases, such as atherosclerosis [23], cardiovascular disease [24], and Alzheimer's disease [25]. Thus, it may be beneficial to quantify and characterize cerebral metabolism in the ISO range, which may provide better insight into neurophysiological mechanisms and discover features that differ between healthy YA and OA for the early diagnosis of Alzheimer's disease and other brain disorders.

1.3. Aim of This Study

Numerous studies have reported differences in brain function in response to different cognitive tasks in the prefrontal cortices of young and older individuals [6,26-28]. For example, healthy aging brains exhibited increases in bilateral activation of the frontal and prefrontal cortices when performing the tasks that stimulated only unilaterally in YA [6]. Studies examining the impact of age on task performance have consistently shown that YA performed better on measures of frontal lobe function than OA, while both groups performed equally well on tasks that do not primarily rely on the frontal lobe [26]. In contrast, this study aimed to identify and quantify the differences between YA and OA in a newly defined set of neurophysiological metrics (i.e., $uCOP_{left}$ and $uCOP_{right}$, $bCON_{HbO}$, and $bCON_{CCO}$) in the resting prefrontal cortex.

The four new neurophysiological metrics can be derived from noninvasive measurements of 2-channel broadband near-infrared spectroscopy (bbNIRS) obtained from the forehead of human participants [8,10,19]. This portable device employs near-infrared light to non-invasively detect changes in chromophore concentrations, encompassing oxidized cytochrome c oxidase (Δ[CCO]) and oxygenated hemoglobin (Δ[HbO]) [29,30]. In this study, we first quantified these four metrics in OA (n=24) at all three ISO (E/N/M) frequencies and then compared them with the respective metrics in YA (n=26), followed by examining possible gender differences within each age group. The aim of this study was to prove our hypothesis that there are significant differences in unilateral metabolic-hemodynamic coupling (uCOP) and bilateral connectivity (bCON) in the prefrontal cortex between YA and OA. Such new findings may be potentially meaningful for clinical applications, since impairment in unilateral/local coupling or bilateral connectivity of prefrontal infraslow oscillations (ISO) may signify neurological disorders [1,8,31].

2. Results

While we completed data acquisition of the bbNIRS measurements under both eyes-open and eyes-closed conditions from the OA group, we focused on the results with eyes-closed measurements to be identical and thus comparable to the measurement conditions for the YA group.

2.1. Bilateral Prefrontal Connectivity of Δ[HbO] and Δ[CCO] in Older and Younger Adults

The bilateral prefrontal connectivity of Δ[HbO] and Δ[CCO] (i.e., $bCON_{HbO}$ and $bCON_{CCO}$) from OA (n=24) and YA (n=26 [8]) in eyes-closed resting state is plotted in Figures 2(a) and 2(b), respectively, for all three E/N/M bands. The coherence values for the pairs representing $bCON_{HbO}$ and $bCON_{CCO}$ are listed in Table 1. Based on two-sample t-tests, YA had a statistically higher coherence ($p<0.001$), and thus stronger connectivity, than OA for the bilateral hemodynamic activities of the prefrontal cortex only in the myogenic frequency band. This significant difference had a very large effect size of 2.35, as listed in Table 1(a). On the other hand, the comparative results of $bCON_{CCO}$ revealed that OA had much stronger metabolic/mitochondrial coherence bilaterally than younger adults in the myogenic band, with a very large effect size of 2.99, as listed in Table 1(b).

Preprints (www.preprints.org) | NOT PEER-REVIEWED | Posted: 29 August 2023 doi:10.20944/preprints202308.1869.v1

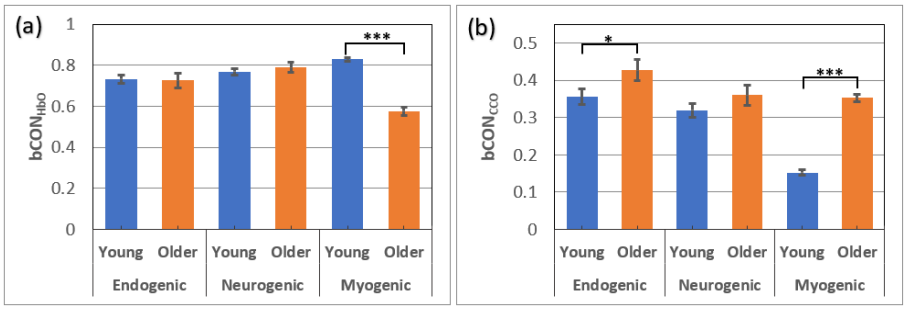

Figure 2. Prefrontal bilateral connectivity of (a) Δ[HbO] and (b) Δ[CCO] in OA (n=24) and YA (n=26) at rest with eyes closed in endogenic (0.005-0.04 Hz), neurogenic (0.04-0.02 Hz), and myogenic (0.02-0.2 Hz) bands. Errors bars represent the standard error of the mean. *: $p < 0.05$; ***: $p < 0.001$.

Note that the $bCON_{HbO}$ and $bCON_{CCO}$ values for YA (n=26) were grand averaged over five visits [8], while OA had only one visit for the measurements (n=24). The outcome of such a difference in the sampling size between the two groups is addressed in the Discussion section.

Table 1. Resting-state prefrontal connectivity of (a) $bCON_{HbO}$ and (b) $bCON_{CCO}$ compared between the OA (n=24) and YA (n=26 [8]) at all three E/N/M bands.

(a) Bilateral hemodynamic connectivity, $bCON_{HbO}$, of the two age groups

Frequency Bands	OA (n = 24)	YA (n = 26)	p values (t-test)	Cohen's d
Endogenic	0.72 ± 0.17	0.73 ± 0.22	0.79	N/A
Neurogenic	0.79 ± 0.12	0.77 ± 0.17	0.59	N/A
Myogenic	0.58 ± 0.10	0.83 ± 0.11	1.1E-12 ***	**2.35**

(b) Bilateral metabolic/mitochondrial connectivity, $bCON_{CCO}$, of the two age groups

Frequency Bands	OA (n = 24)	YA (n = 130)	p values (t-test)	Cohen's d
Endogenic	0.43 ± 0.14	0.36 ± 0.25	0.023*	**0.37**
Neurogenic	0.36 ± 0.14	0.32 ± 0.21	0.1625	N/A
Myogenic	0.35 ± 0.04	0.15 ± 0.08	1.1E-21***	**2.99**

*: It marks a significant difference between OA and YA at the significance level of $p<0.05$. ***: It marks a significant difference between OA and YA at the significance level of $p<0.001$.

Although the results presented above were based on 7-min eyes-closed measurements for comparing values of $bCON_{HbO}$ and $bCON_{CCO}$ between the two age groups, the data taken from the 7-min eyes-open measurements of OA were also analyzed and presented in Section B of the Supplementary Materials. Paired t-tests demonstrated that there was no significant difference in any respective bCON parameter beween the eyes-closed and eyes-open measurements in the OA group.

2.2. Unilateral Prefrontal Coupling between Δ[HbO] and Δ[CCO] in Older and Younger Adults

The same coherence analysis was performed to find the unilateral hemodynamic-mitochondrial coupling on the left and right side of the prefrontal cortex from OA (n=24) and YA (n=26 [8]) in eyes-closed resting state. The results are plotted in Figures 3(a) and 3(b) for all three E/N/M bands. Accordingly, the coherence values for either side of $uCOP_{left}$ and $uCOP_{right}$ for each age group are listed in Table 2. As shown in Figure 3, OA exhibited significantly larger coherence between Δ[HbO] and Δ[CCO] oscillations in all three frequency bands, indicating stronger mitochondrial–haemodynamic couplings on either side of the prefrontal cortex (i.e. $uCOP_{left}$ and $uCOP_{right}$) than younger adults. In particular, such unilateral coupling on both lateral sides of the OA was much stronger in the myogenic frequency band than in the YA group, with very large effect sizes of 1.96 and 2.72 (seeTable 2). Unilateral coupling strengths at the endogenic and neurogenic frequency bands

Preprints (www.preprints.org) | NOT PEER-REVIEWED | Posted: 29 August 2023 doi:10.20944/preprints202308.1869.v1

in the OA group were significantly larger with a medium effect size (0.5-0.8) than those in the YA group (Table 2).

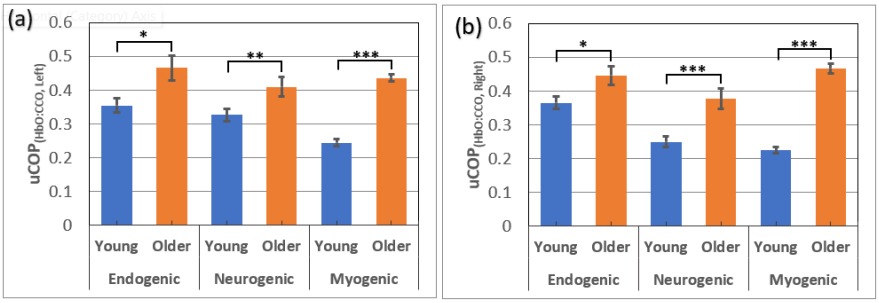

Figure 3. Unilateral coupling between Δ[HbO] and Δ[CCO] on the (a) left and (b) right prefrontal cortex compared between OA (n=24) and YA (n=26 [8]) at rest with eyes closed in all three E/N/M bands. Errors bars represent the standard error of the mean. **: $p < 0.05$; ***:* $p < 0.001$.

Table 2. Unilateral coupling between Δ[HbO] and Δ[CCO] on the (a) left and (b) right prefrontal cortex compared between OA (n=24) and YA (n=26 [8]) at all three E/N/M bands.

(a) Unilateral coupling on the left prefrontal cortex, $uCON_{left}$, of two age groups

Frequency Bands	OA (n = 24)	YA (n = 26)	p values (t-test)	Cohen's d
Endogenic	0.47 ± 0.19	0.35 ± 0.24	0.011*	**0.536**
Neurogenic	0.41 ± 0.14	0.33 ± 0.21	0.0098**	**0.508**
Myogenic	0.44 ± 0.06	0.24 ± 0.12	1.4E-18***	**1.96**

(b) Unilateral coupling on the right prefrontal cortex, $uCON_{right}$, of two age groups

Frequency Bands	OA (n = 24)	YA (n = 26)	p values (t-test)	Cohen's d
Endogenic	0.45 ± 0.14	0.36 ± 0.21	0.023*	**0.44**
Neurogenic	0.38 ± 0.15	0.25 ± 0.17	0.0007***	**0.78**
Myogenic	0.47 ± 0.07	0.22 ± 0.11	3.9E-18***	**2.72**

*: It marks a significant difference between OA and YA at the significance level of $p<0.05$. **: It marks a significant difference between OA and YA at the significance level of $p<0.01$. ***: It marks a significant difference between OA and YA at the significance level of $p<0.001$.

Similar to the case for the bCON calculations, the values of uCOP derived from the 7-min eyes-open measurements of OA were also analyzed and are presented in Section B of the Supplementary Materials. Paired t-tests demonstrated no significant difference in any respective uCOP parameter between eyes-closed and eyes-open measurements in the AO group.

2.3. Gender Difference in Bilateral Connectivity of Unilateral Coupling

Besides examining the age difference in resting state bCON and uCOP in the prefrontal cortex of healthy adults, it is also interesting and meaningful to inspect the gender difference in those respective bCON and uCOP metrics within each OA and YA groups. Accordingly, we quantified such metrics within each age group in all three E/N/M bands, as shown in Figure 4. Detailed coherence values of bCON and uCOP metrics as well as p values of two-sample t-tests for gender comparisons can be found in Section C of the Supplementary Materials. Figure 4 and statistical analysis results clearly revealed that the gender difference in bilateral connectivity and unilateral mitochondrial-hemodynamic coupling was non-significant for most of the metrics, within each age group.

Preprints (www.preprints.org) | NOT PEER-REVIEWED | Posted: 29 August 2023 doi:10.20944/preprints202308.1869.v1

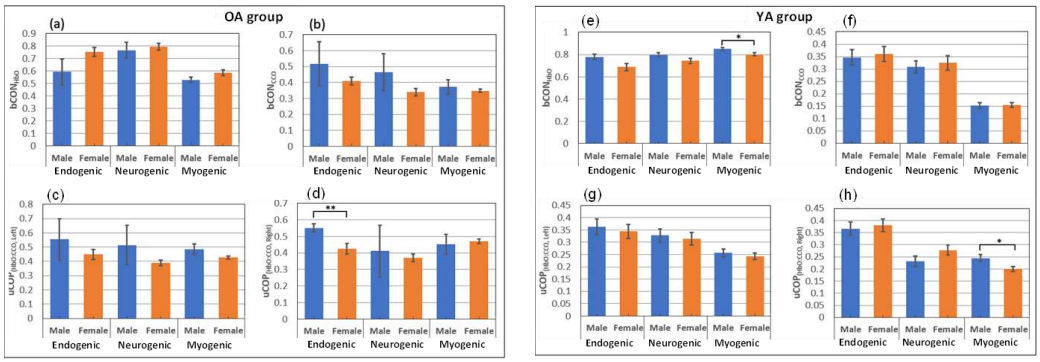

Figure 4. Gender comparison of prefrontal bilateral connectivity and unilateral coupling within the OA group (males=4; females=20) for (a) $bCON_{HbO}$, (b) bCONCCO, (c) $uCOP_{left}$, and (d) $uCOP_{right}$ over the E/N/M bands. In the similar way, gender comparisons within the YA group (males=14; females=12) for (e) $bCON_{HbO}$, (f) bCONCCO, (g) $uCOP_{left}$, and (h) $uCOP_{right}$ over the E/N/M bands. Errors bars are the standard error of the mean. *: $p < 0.05$; **: $p < 0.01$;.

3. Discussion

The experimental results shown in Section 2 revealed three key findings. First, YA had significantly stronger bilateral hemodynamic connectivity ($bCON_{HbO}$), as represented by temporal coherence of resting HbO in the M band (Table 1) than its counterpart, OA with a very large effect size (=2.35). Second, on the other hand, OA had significantly stronger bilateral metabolic connectivity ($bCON_{CCO}$) in the M band than YA, also with a very large effect size (=2.99). Third, OA also had significantly stronger unilateral coupling on both prefrontal sides ($uCOP_{left}$ and $uCOP_{right}$) in all three E/N/M bands, with very large effect sizes for M band (> 1.9) and a medium effect size for E/N bands (0.4 < effect size < 0.8). All these results clearly proved our hypothesis that there are significant differences in unilateral metabolic-hemodynamic coupling (uCOP) and bilateral connectivity (bCON) in the prefrontal cortex between YA and OA groups.

3.1. Age Effect on Bilateral Hemodynamic Connectivity of the Resting Prefrontal Cortex

Figure 2(a) and Table 1(a) demonstrate that both YA and OA had strong bilateral hemodynamic connectivity in all three E/N/M oscillation bands, with $bCON_{HbO}$ larger than 0.7, except for OA in the M band. It is known that cerebral blood vessel walls in the human brain oscillate in infraslow rhythms in all three E/N/M bands [13,14] [15,16]**.** Thus, this set of results was expected that the hemodynamic coherence/connectivity between the two lateral prefrontal cortices would be large in both age groups. However, the OA group exhibited significantly weaker connectivity in the M band than the YA group. This implies that the synchrony between the smooth muscle cells covering the vascular walls on both lateral sides of the prefrontal cortex is lower in older participants than in younger participants. We speculated that this age effect could be attributed to the aging smooth muscle cells of the cerebral blood vessels that become less elastic and have reduced oscillation frequencies [8]. However, synchronized hemodynamic activity in both E and N bands, mediated by endothelial cells and interneurons, remained unaffected by age. Note that our interpretation of the reduction in bilateral connectivity in the M band in OA is consistent with a previous connectivity study [32]. According to Li et al. [32], OA showed an overall decline in both global and local network efficiency compared with YA. In addition, YA showed an abundance of brain network hubs in the prefrontal cortex, whereas OA showed hub shifts to the sensorimotor cortex.

3.2. Age Effect on Bilateral Metabolic Connectivity of the Resting Prefrontal Cortex

We introduced the concept of bilateral metabolic connectivity in the resting prefrontal cortex and quantified it in all three E/N/M bands in young participants in Ref. **[8]**. In this study, we compared these quantities of 24 OA with those of 26 YA **[8]**, as presented in Figure 2(b) and Table

1(b). Our observations included (1) that both age groups had much smaller bilateral mitochondrial connectivity ($bCON_{CCO}$ being 0.3-0.4) than values of $bCON_{HbO}$ (being 0.7-0.8) in all three E/N/M bands, and (2) that YA had significantly weaker $bCON_{CCO}$ values than OA in the M band with a very large effect size (=2.99). Observation (1) is expected because cerebral mitochondrial activity reflected by the redox state of CCO occurs more locally on each lateral side of the prefrontal cortex and thus is less synchronized between the two sides in all three frequency bands. Observation (2), however, reveals that the prefrontal cortex of YA operates more independently between the two lateral sides for localized cerebral metabolism with much less bilateral synchrony in the M band than OA. This may imply that as people age, bilateral prefrontal synchronization of cerebral metabolism increases along with the oscillation of smooth muscle cells of blood vessels. Thus, $bCON_{CCO}$ in the M band is highly age-dependent and may be an excellent candidate to serve as a marker for age-related brain state conditions.

3.3. Age Effect on unilateral Metabolic-hemodynamic Coupling of the Resting Prefrontal Cortex

The next metric showing a significant age effect was the unilateral hemodynamic-mitochondrial coupling (uCOP) on the two lateral sides of the forehead. Overall, OA exhibited significantly stronger unilateral coupling on both lateral sides ($uCOP_{left}$ and $uCOP_{right}$) in all three E/N/M bands (Figure 3), with a medium effect size for the E and N bands ($0.4 <$ effect size < 0.8) and a very large effect size for the M band (> 1.9) (see Table 2). Note that the values of $uCOP_{left}$ and $uCOP_{right}$ in OA were almost twice as large as those in YA. The neurophysiological measure of uCOP reflects the mitochondrial-vascular or metabolic-hemodynamic interactivity on each individual prefrontal side. Furthermore, the uCOP value signifies direct coupling or the relationship between metabolic demand and blood supply. Accordingly, our results imply that OA has significantly tighter relationships between local mitochondrial activity (reflected by the redox state of CCO) and oxygenated blood supply (revealed by HbO signals). In other words, the prefrontal cortex in OA needs to have a faster or better supply-to-demand chain in the cerebral substrate than that in YA to maintain active and normal prefrontal function in the resting state. This interpretation seems to work for all three frequency bands, while such neurophysiological coupling is strongest with smooth muscles in the M band for the OA group.

3.4. Signals Measured under Eyes-Open and Eyes-Closed Conditions

It is known that the resting human brain often exhibits different EEG temporal and spatial signal patterns when the measurement is taken with eyes open or closed. However, it was unknown whether prefrontal hemodynamic and/or metabolic measurements would differ under eyes-open or eyes-closed conditions. This study clearly indicated that none of the bilateral connectivity metrics (i.e., $bCON_{HbO}$ and $bCON_{CCO}$) or unilateral metabolic-hemodynamic coupling ($uCOP_{left}$ and $uCOP_{right}$) in all three E/N/M bands showed any significant difference under either eyes-open or eyes-closed measurement conditions (Section B in the Supplementary Materials). This observation experimentally confirms that the prefrontal neurophysiological metrics of a resting brain can be measured with either eyes open or eyes closed without any significant impact on the results. This finding provides practical and helpful guidance for future experimental designs.

3.5. Gender Difference in Resting Bilateral Connectivity and Unilateral Coupling

Although our results showed age effects on both bCON and uCOP in all three E/N/M bands, we wondered whether these metrics would have a gender effect. Subsequently, for each age group, we conducted two-sample t-tests to investigate the potential gender differences for each of the uCOP and bCON metrics. However, no significant evidence was found within each age group for most of the metrics, as shown in Figure 4, except for one of the 12 metrics in OA and two of the 12 metrics in YA. Specifically, we observed that older males had a significantly higher $uCOP_{right}$ value in the E band than older females with a large effect size (0.96). In addition, young males showed significantly higher $uCOP_{right}$ and $bCON_{HbO}$ values in the M band than young females, with a small to medium effect size

 doi:10.20944/preprints202308.1869.v1

(see Section C in the Supplementary Materials). Overall, our results demonstrated minor or non-significant sex differences in prefrontal bCON and uCOP in all three E/N/M bands in each age group. However, the sample size for older males was very small (=4); therefore, the statistical comparison within the OA group would be less robust, which will be addressed in future work.

3.6. Limitations of the Study and Future Work

While this study provides several new and key findings, it has several limitations. First, the measurements from OA were obtained from one visit, but the data from YA were derived and averaged from five visits. Second, during the first visit, it was unavoidable for some of the OA to be anxious at different levels because of the unfamiliarity of the environment and experimental setup. Such anxiety could cause motion artifacts and mental nervousness and thus lead to extra noise during bbNIRS data acquisition. Third, the sample size was limited to older males. Regarding data analysis, MTM is a relatively complex algorithm that is more appropriate for EEG data analysis, but it may not be necessary for bbNIRS analysis. Moreover, our current data analysis could not discriminate signal contamination from the superficial layers (i.e., scalp and skull) of the human forehead.

For future improvement, for the first limitation, we can perform a more rigorous statistical analysis, such as the boot-strapping permutation test or the analysis of variance (ANOVA), to consider both between-group and within-group factors for the currently available data. In addition, it will be advantageous to perform future measurements with two visits or to have a practice session for OA to reduce anxiety. We need to make all possible efforts to recruit more male OA for a balanced sample size for robust gender effect analysis. Regarding the improvement in data analysis, the Welch method [33] can be a simpler approach for performing bbNIRS spectral analysis. Finally, it is necessary to learn and implement appropriate preprocessing algorithms for bbNIRS spectral data [34] to remove possible contamination of extracranial layers for more accurate results.

4. Materials and Methods

4.1. Participants

This study employed a between-group experimental design with two age groups. Twenty-six healthy YA (14 males and 12 females; mean ± SD age = 22.4 ± 2.3 years) were recruited from the university community and reported in a recent publication [1]. For this study, each young participant had 5 visits, separated by at least 7 days. They were screened using the same inclusion/exclusion criteria as those used in previous studies [11,35]. In addition, we recruited 24 OA (4 males and 20 females; mean ± SD age = 67.2 ± 5.9 years) from the Dallas-Fort Worth community and were screened with the following inclusion criteria: (1) aged 55 years or older, (2) not experiencing cognitive impairment or decline, and (3) being able to travel without assistance to the research laboratory on UT Arlington campus. Those who had brain injuries or surgeries within the past year or could not provide consent of their own were excluded from the healthy subject category. Experimental procedures (see below) were approved by the Institutional Review Board of the University of Texas at Arlington. All measurements were conducted after obtaining informed consent. The participants were compensated for their time.

4.2. Experiment Protocol and Setup

Both age groups underwent the same experimental protocol with the same experimental setup, which was reported in detail in ref. [1]. For the reader's convenience, we briefly summarize the experimental protocol and setup as follows. Each OA was asked to complete a demographic questionnaire and sign a consent form, followed by sitting comfortably on a sofa chair. As shown in Figures 5(a) and 5(b), a 2-channel bbNIRS headset was positioned bilaterally on the participant's foreheads, along with a 19-channel EEG cap. After the completion of bbNIRS+EEG setup, each measurement took 14 min readings while the participant was in resting state with eyes open and closed for 7 min each. After completion of the 14-min data collection, only 2-channel bbNIRS data were used for further data processing for this study.

Preprints (www.preprints.org) | NOT PEER-REVIEWED | Posted: 29 August 2023 doi:10.20944/preprints202308.1869.v1

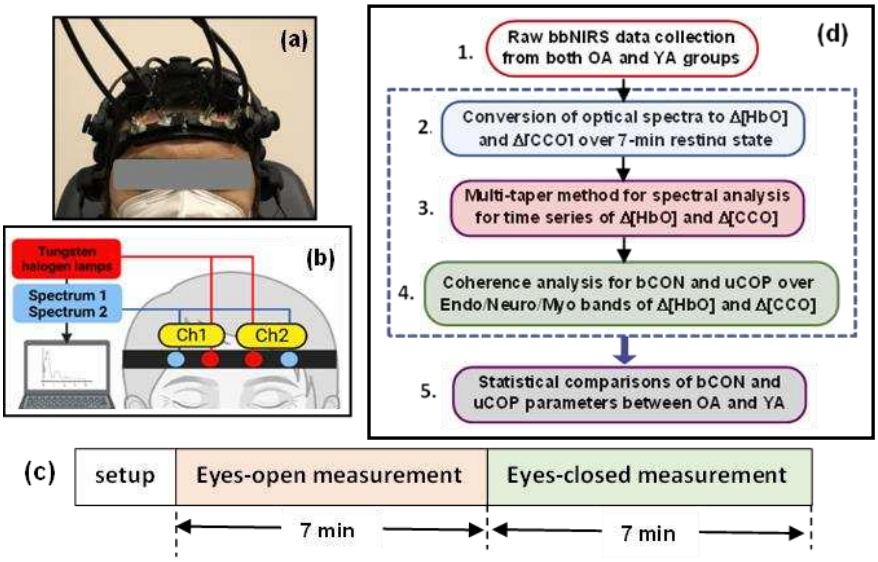

Figure 5. (a) Photograph of a human participant wearing a 2-channel bbNIRS headset on the forehead along with a 19-channel EEG cap. (b) Schematic diagram depicting the 2-channel bbNIRS setup, including two spectrometers as optical detectors, two tungsten-halogen lamps as light sources, two sets of optical fiber probes, and a control/acquisition computer. (c) The measurement protocol which consisted of 7-min eyes open and 7-min eyes closed measurements. It was followed similarly for both the YA and OA studies. (d) Five-step flow chart for data analysis, which enables to quantify bilateral connectivity and unilateral coupling of mitochondrial and hemodynamic activity at rest in the three E/N/M frequency bands (see text for details). Steps 2 to 4 (outlined by the dashed box) were repeated for both age groups, enabling statistical comparisons between them.

4.3. Broadband Near-Infrared Spectroscopy and its Measurements

As shown in Figure 5(b) and Refs. [8,10], the bbNIRS system employed in this study was designed with two channels to collect data concurrently from each lateral forehead of the participant. The two light sources used were halogen lamps (OSL2IR, Thorlabs, Inc., NJ, USA) emitting broadband white light. Two CCD array spectrometers (QEPRO; Ocean Optics Inc., Orlando, FL, USA) were used for spectroscopic detection. An integration time of 1.5 sec (i.e., a sampling rate of 0.67 Hz) was set to balance the temporal resolution and adequate signal strength. Two sets of optical fiber probes were connected to a laptop computer that controlled the data acquisition, displayed the results, and stored the data for the offline process. Calibration of the two spectrometers was performed using an ink-intralipid phantom, demonstrating identical spectral quantifications from both channels.

To ensure proper placement, optical fibers connected the lamps and detectors to a 3-D printed headband, as seen in Figures 5(a) and 5(b). The headband was secured to each participant's forehead using Velcro straps and medical tapes applied to the probe-skin interface to stabilize the probe without causing discomfort to the participants. In addition, this stabilization greatly reduces motion artefacts. This headband was specifically designed with divots to accommodate the EEG prefrontal electrodes while securing the placement of the bbNIRS system on the subject's forehead. The source and detector separation for each channel was 3 cm. This setup enables the simultaneous measurement of optical spectral alterations in both the left and right foreheads of healthy participants in the resting state [8].

In the meantime, a compact electroencephalogram (EEG) device with a dry, blue-tooth controlled, 19-channel headset (Quick-20, CGX Systems, San Diego, CA, USA) was employed for concurrent dual-mode measurements. However, the focus of this study was on the results only from the bbNIRS of the two age groups, leaving the investigation of EEG in a future study.

4.4. Data Analysis

Preprints (www.preprints.org) | NOT PEER-REVIEWED | Posted: 29 August 2023 doi:10.20944/preprints202308.1869.v1

The algorithm developed to analyze 2-channel bbNIRS data for the quantification of bilateral connectivity of ΔHbO and ΔCCO, as well as unilateral mitochondrial-hemodynamic coupling, of the human forehead was recently introduced [1] and applied to the investigation of prefrontal responses to noninvasive light stimulation [10,19]. The detailed data analysis can be summarized in five steps, as shown in Figure 5(d). While complete derivation and explanation of the algorithm can be found in Refs. [1,2], we briefly describe the five steps below for the convenience of readers.

Step 1: Raw bbNIRS data collection from both OA and YA groups

For both OA and YA experiments, the recorded data by both spectrometers were a set of optical spectra at different times (t), as expressed $I(t, \lambda)$. A relative optical density spectrum, ΔOD(t, λ), can be defined and calculated at each wavelength λ as:

$$\Delta OD(t,\lambda) = log_{10}[\frac{I_0(t=0,\lambda)}{I(t,\lambda)}], \quad (1)$$

where $I_0(t=0, \lambda)$ is the baseline spectrum at time t=0 or an average of several initial baseline spectral readings, and $I(t, \lambda)$ represents time-varying spectra acquired at each time point throughout the entire experiment.

Step 2: Conversion of ΔOD(t, λ) to Δ[HbO](t, λ) and Δ[CCO](t, λ) over 7-min resting state

With a sample rate of 0.67 Hz, 7-min bbNIRS data collection provided a set of 280 spectra for either eyes-open or eyes-closed session. The recorded spectrum was in the wavelength range of 740 to 1100 nm, but a spectral band of 780 to 900 nm was sufficient for our need [36]. According to the modified Beer-Lambert law, we converted ΔOD(t, λ) to Δ[HbO](t, λ) and Δ[CCO](t, λ) [37-39] for each time point over the 7-min measurement window for both lateral sides of the measurements [8,11,19]. Section D in the Supplementary Materials provides theoretical/mathematical derivations in detail for this step.

Step 3: Spectral analysis of Δ[HbO](t, λ) and Δ[CCO](t, λ)

To perform spectral analysis for time series of Δ[HbO] and Δ[CCO], we used the multi-taper method (MTM) [8,40,41]. This method facilitates frequency spectra for both Δ[HbO] and Δ[CCO] with relatively high spectral resolution and low noise using Slepian sequences to taper time series in the time domain followed by the fast Fourier transform. Specifically, several functions available in the FieldTrip toolbox (including "ft_freqanalysis") were performed for MTM operation on the MATLAB platform [42,43]. The decomposed amplitude and phase were achieved as a complex number that was further used in the coherence quantification (see Step 4). See Section E in the Supplementary Materials for a graphical explanation for the function of "ft_freqanalysis."

Step 4: Hemodynamic and metabolic connectivity/coupling quantification [8,10]

Connectivity analysis, in principle, estimates the level by which two time series oscillate synchronously. One of the widely used connectivity measures is coherence, a phase-based frequency-domain analysis that is quantified as a normalized value between 0 and 1. Mathematically, the representation of coherence (COH) between two time series for a specific frequency of ω is

$$coh_{xy}(\omega) = \frac{[S_{xy}(\omega)]}{\sqrt{S_{xx}(\omega)S_{yy}(\omega)}} \quad (2)$$

where Sxx and Syy are the power estimates of signals x and y, and Sxy is the averaged cross spectral density of the two data series [44]. These terms are calculated using the complex values obtained from the MTM method [41,45] (see Step 3 above). The flow chart shown in Section E in the Supplementary Materials also illustrates the function of "ft_connectivityanalysis" graphically for an easy understanding of the calculation.

In this study, we utilized several functions in MATLAB (including "ft_connectivityanalysis") available in the FieldTrip toolbox to perform coherence operations. Specifically, we calculated coherence values for the following four pairs of measured Δ[HbO] and Δ[CCO] signals: (1) bilateral hemodynamic connectivity between $\Delta[HbO]_{right}$ and $\Delta[HbO]_{left}$ (i.e., $bCON_{HbO}$), (2) bilateral metabolic connectivity between $\Delta[CCO]_{right}$ and $\Delta[CCO]_{left}$ ($bCON_{CCO}$), (3) unilateral hemodynamic-metabolic coupling on the ipsilateral side between $\Delta[HbO]_{right}$ and $\Delta[CCO]_{right}$ ($uCOP_{right}$), and (4) unilateral

Preprints (www.preprints.org) | NOT PEER-REVIEWED | Posted: 29 August 2023 doi:10.20944/preprints202308.1869.v1

hemodynamic-metabolic coupling on the contralateral side between $\Delta[HbO]_{left}$ and $\Delta[CCO]_{left}$ ($uCOP_{left}$). These calculations were performed separately for the three frequency bands (E/N/M).

Step 5: Statistical Analysis

After the aforementioned parameters at each E/N/M band were quantified for OA, we performed two-sample t-tests between the OA and YA groups to determine whether each of the bCON and uCOP parameters was age-dependent. The significance level was set at $p<0.05$. All respective values for the YA group were based on the results reported in Ref. [8]. When a significant difference between the two groups was obtained, we further calculated Cohen's d to assess the effect size of statistical significance. Accordingly, $0.2 < d < 0.5$, $0.5 < d < 0.8$, $0.8 < d < 1.3$, and $d > 1.3$ are considered small, medium, large, and very large effect sizes, respectively.

Furthermore, within each age group, we performed two-sample t-tests between male and female participants to examine the gender difference for each of the quantified connectivity and coupling parameters.

To visualize the five steps in data processing, Figure 6 below illustrates representative data or outcome after each step: the figure in Step 1 shows group-averaged raw bbNIRS optical spectra; the figure in Step 2 displays a quantified time series of Δ[HbO] with a broad frequency range in < 0.25 Hz; the figures in Step 3 include a spectral analysis plot after MTM along with time series in three E/N/M bands; Step 4 lists the quantities for coherence calculations for all three E/N/M bands; and Step 5 shows an example for statistical comparisons between the two age groups.

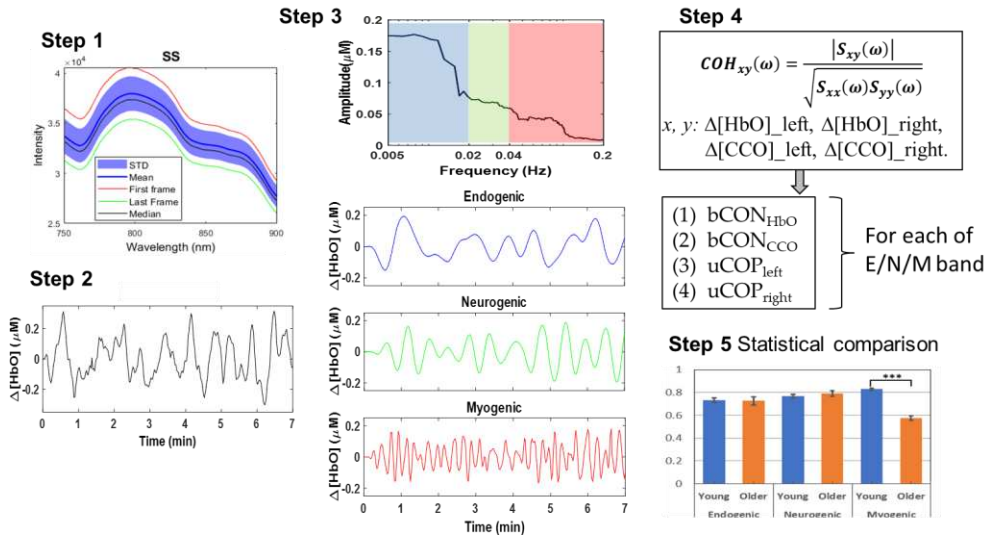

Figure 6. Step 1: An assortment of raw optical spectra acquired using bbNIRS, averaged over a 7-minute collection time. The mean and median spectra are represented by shading with standard deviation and outlined by the highest and lowest spectra. Step 2: This panel exhibits a 7-min time series of Δ[HbO] from a random participant as an example. Step 3: A quantified spectral amplitude of Δ[HbO] is presented after multi-taper spectral analysis was employed. The E/N/M frequency bands are marked by blue, green, and red boxes, respectively. Accordingly, the frequency-decomposed time series of the spectral curve are obtained in respective E/N/M bands. Step 4: It graphically illustrates the quantification of coherence for four pairs of Δ[HbO] and Δ[CCO] on each lateral side in each E/N/M band. Step 5: It graphically illustrates statistical comparisons between the two age groups for respective parameters.

5. Conclusions

In this study, we hypothesized that there would be significant differences in unilateral metabolic-hemodynamic coupling and bilateral connectivity in the prefrontal cortex between YA and OA. To test this hypothesis, we performed noninvasive prefrontal measurements from 24 OA using the same 2-channel bbNIRS setup and 14-min resting-state experimental protocol as those reported

in *[8]* from 26 YA. After comprehensive quantification of both uCOP and bCON at all three E/N/M frequencies and careful statistical comparisons, we demonstrated that YA had significantly stronger bilateral hemodynamic connectivity in the M band than OA with a very large effect size, whereas OA had significantly stronger bilateral metabolic connectivity in the M band than YA also with a very large effect size. Furthermore, the OA exhibited significantly stronger unilateral coupling on both prefrontal sides in all three E/N/M bands, particularly with a very large effect size in the M band (> 1.9). All these results can be interpreted by neurophysiological principles while unambiguously supporting our hypothesis. The framework reported in this paper has demonstrated that the neurophysiological metrics of prefrontal uCOP and bCON are highly age-related and may have the potential to serve as neurophysiological features of human brain health that can be translatable for future clinical applications, such as for early detection or identification of age-associated neurological disorders including Alzheimer's disease.

Supplementary Materials: The following supporting information can be downloaded at the website of this paper posted on Preprints.org

Author Contributions: Conceptualization, K.L. and H.L.; methodology, C.S., F. S., K.K., and C. C.; software, S.S. and H.L.; validation, C.S., F.S., and S.S.; formal analysis, C.S., F.S., C.C., and H.L.; resources, K.K., K.L., and H.L.; data curation, C.S., F. S., and C. C.; writing—original draft preparation, C.S., F. S., and C. C.; writing—review and editing, all authors; visualization, C.S., F. S., and C. C., and H.L.; supervision, K.L. and H.L.; project administration, H.L.; funding acquisition, K.L. and H.L. All authors have read and agreed to the published version of the manuscript.

Funding: This research was funded in part by the NIA (R21AG079309) and the NIMH (RF1MH114285) of the National Institutes of Health.

Institutional Review Board Statement: The study was conducted according to the guidelines of the Declaration of Helsinki and approved by the Institutional Review Board of the University of Texas at Arlington (IRB protocol #2022-0213, approved on June 23, 2022).

Informed Consent Statement: Informed consent was obtained from all subjects involved in the study.

Data Availability Statement: The data presented in this study are available on request from the corresponding author.

Conflicts of Interest: The authors declare no conflict of interest.

References

1. Motzkin, J.C.; Newman, J.P.; Kiehl, K.A.; Koenigs, M. Reduced prefrontal connectivity in psychopathy. *J Neurosci* **2011**, *31*, 17348-17357. https://doi.org/10.1523/JNEUROSCI.4215-11.2011.
2. Racz, F.S.; Mukli, P.; Nagy, Z.; Eke, A. Increased prefrontal cortex connectivity during cognitive challenge assessed by fNIRS imaging. *Biomed Opt Express* **2017**, *8*, 3842-3855. https://doi.org/10.1364/BOE.8.003842.
3. Yu, J.W.; Lim, S.H.; Kim, B.; Kim, E.; Kim, K.; Kyu Park, S.; Seok Byun, Y.; Sakong, J.; Choi, J.W. Prefrontal functional connectivity analysis of cognitive decline for early diagnosis of mild cognitive impairment: a functional near-infrared spectroscopy study. *Biomed Opt Express* **2020**, *11*, 1725-1741. https://doi.org/10.1364/BOE.382197.
4. Jobson, D.D.; Hase, Y.; Clarkson, A.N.; Kalaria, R.N. The role of the medial prefrontal cortex in cognition, ageing and dementia. *Brain Commun* **2021**, *3*, fcab125. https://doi.org/10.1093/braincomms/fcab125.
5. Sampath, D.; Sathyanesan, M.; Newton, S.S. Cognitive dysfunction in major depression and Alzheimer's disease is associated with hippocampal–prefrontal cortex dysconnectivity. *Neuropsychiatric Disease and Treatment* **2017**, *13*, 1509.
6. Grady, C. The cognitive neuroscience of ageing. *Nat Rev Neurosci* **2012**, *13*, 491-505. https://doi.org/10.1038/nrn3256.
7. Jones, L.K. Neurophysiological development across the life span. *American Counseling Association* 2017, pp. 27-44.
8. Shahdadian, S.; Wang, X.; Kang, S.; Carter, C.; Chaudhari, A.; Liu, H. Prefrontal cortical connectivity and coupling of infraslow oscillation in the resting human brain: a 2-channel broadband NIRS study. *Cereb Cortex Commun* **2022**, *3*, tgac033. https://doi.org/10.1093/texcom/tgac033.
9. Swami, S. Executive functions and decision making: A managerial review. *IIMB Management Review* **2013**, *25*, 203-212. https://doi.org/.

10. Shahdadian, S.; Wang, X.; Kang, S.; Carter, C.; Liu, H. Site-specific effects of 800- and 850-nm forehead transcranial photobiomodulation on prefrontal bilateral connectivity and unilateral coupling in young adults. *Neurophotonics* **2023**, *10*, 025012. https://doi.org/10.1117/1.NPh.10.2.025012.
11. Wang, X.; Tian, F.; Reddy, D.D.; Nalawade, S.S.; Barrett, D.W.; Gonzalez-Lima, F.; Liu, H. Up-regulation of cerebral cytochrome-c-oxidase and hemodynamics by transcranial infrared laser stimulation: A broadband near-infrared spectroscopy study. *J Cereb Blood Flow Metab* **2017**, *37*, 3789-3802. https://doi.org/10.1177/0271678X17691783.
12. Obrig, H.; Wenzel, R.; Kohl, M.; Horst, S.; Wobst, P.; Steinbrink, J.; Thomas, F.; Villringer, A. Near-infrared spectroscopy: does it function in functional activation studies of the adult brain? *Int J Psychophysiol* **2000**, *35*, 125-142. https://doi.org/10.1016/s0167-8760(99)00048-3.
13. Stefanovska, A.; Bracic, M.; Kvernmo, H.D. Wavelet analysis of oscillations in the peripheral blood circulation measured by laser Doppler technique. *IEEE Trans Biomed Eng* **1999**, *46*, 1230-1239. https://doi.org/10.1109/10.790500.
14. Bracic, M.; Stefanovska, A. Wavelet-based analysis of human blood-flow dynamics. *Bull Math Biol* **1998**, *60*, 919-935. https://doi.org/10.1006/bulm.1998.0047.
15. Vermeij, A.; Meel-van den Abeelen, A.S.; Kessels, R.P.; van Beek, A.H.; Claassen, J.A. Very-low-frequency oscillations of cerebral hemodynamics and blood pressure are affected by aging and cognitive load. *Neuroimage* **2014**, *85 Pt 1*, 608-615. https://doi.org/10.1016/j.neuroimage.2013.04.107.
16. Bernjak, A.; Clarkson, P.B.; McClintock, P.V.; Stefanovska, A. Low-frequency blood flow oscillations in congestive heart failure and after beta1-blockade treatment. *Microvasc Res* **2008**, *76*, 224-232. https://doi.org/10.1016/j.mvr.2008.07.006.
17. Hillman, E.M.C. Coupling Mechanism and Significance of the BOLD Signal: A Status Report. *Annual Review of Neuroscience* **2014**, *37*, 161-181. https://doi.org/10.1146/annurev-neuro-071013-014111.
18. Kvernmo, H.D.; Stefanovska, A.; Kirkeboen, K.A.; Kvernebo, K. Oscillations in the human cutaneous blood perfusion signal modified by endothelium-dependent and endothelium-independent vasodilators. *Microvasc Res* **1999**, *57*, 298-309. https://doi.org/10.1006/mvre.1998.2139.
19. Wang, X.; Ma, L.C.; Shahdadian, S.; Wu, A.; Truong, N.C.D.; Liu, H. Metabolic Connectivity and Hemodynamic-Metabolic Coherence of Human Prefrontal Cortex at Rest and Post Photobiomodulation Assessed by Dual-Channel Broadband NIRS. *Metabolites* **2022**, *12*. https://doi.org/10.3390/metabo12010042.
20. Wiedeman, M.P. Effect of venous flow on frequency of venous vasomotion in the bat wing. *Circ Res* **1957**, *5*, 641-644. https://doi.org/10.1161/01.res.5.6.641.
21. Buerk, D.G.; Riva, C.E. Vasomotion and spontaneous low-frequency oscillations in blood flow and nitric oxide in cat optic nerve head. *Microvasc Res* **1998**, *55*, 103-112. https://doi.org/10.1006/mvre.1997.2053.
22. Zhao, Y.; Vanhoutte, P.M.; Leung, S.W. Vascular nitric oxide: Beyond eNOS. *J Pharmacol Sci* **2015**, *129*, 83-94. https://doi.org/10.1016/j.jphs.2015.09.002.
23. Vita, J.A.; Keaney, J.F., Jr. Endothelial function: a barometer for cardiovascular risk? *Circulation* **2002**, *106*, 640-642. https://doi.org/10.1161/01.cir.0000028581.07992.56.
24. Deanfield, J.E.; Halcox, J.P.; Rabelink, T.J. Endothelial function and dysfunction: testing and clinical relevance. *Circulation* **2007**, *115*, 1285-1295. https://doi.org/10.1161/CIRCULATIONAHA.106.652859.
25. Di Marco, L.Y.; Farkas, E.; Martin, C.; Venneri, A.; Frangi, A.F. Is vasomotion in cerebral arteries impaired in Alzheimer's disease? *Journal of Alzheimer's Disease* **2015**, *46*, 35-53.
26. West, R.L. An application of prefrontal cortex function theory to cognitive aging. *Psychol Bull* **1996**, *120*, 272-292. https://doi.org/10.1037/0033-2909.120.2.272.
27. Cazzell, M.; Li, L.; Lin, Z.J.; Patel, S.J.; Liu, H. Comparison of neural correlates of risk decision making between genders: an exploratory fNIRS study of the Balloon Analogue Risk Task (BART). *NeuroImage* **2012**, *62*, 1896-1911. https://doi.org/10.1016/j.neuroimage.2012.05.030.
28. Li, L.; Cazzell, M.; Zeng, L.; Liu, H. Are there gender differences in young vs. aging brains under risk decision-making? An optical brain imaging study. *Brain Imaging Behav* **2017**, *11*, 1085-1098. https://doi.org/10.1007/s11682-016-9580-z.
29. de Roever, I.; Bale, G.; Cooper, R.J.; Tachtsidis, I. Functional NIRS Measurement of Cytochrome-C-Oxidase Demonstrates a More Brain-Specific Marker of Frontal Lobe Activation Compared to the Haemoglobins. *Adv Exp Med Biol* **2017**, *977*, 141-147. https://doi.org/10.1007/978-3-319-55231-6_19.
30. Pruitt, T.; Carter, C.; Wang, X.; Wu, A.; Liu, H. Photobiomodulation at Different Wavelengths Boosts Mitochondrial Redox Metabolism and Hemoglobin Oxygenation: Lasers vs. Light-Emitting Diodes In Vivo. *Metabolites* **2022**, *12*. https://doi.org/10.3390/metabo12020103.
31. Sampath, D.; Sathyanesan, M.; Newton, S.S. Cognitive dysfunction in major depression and Alzheimer's disease is associated with hippocampal-prefrontal cortex dysconnectivity. *Neuropsychiatr Dis Treat* **2017**, *13*, 1509-1519. https://doi.org/10.2147/NDT.S136122.
32. Li, L.; Babawale, O.; Yennu, A.; Trowbridge, C.; Hulla, R.; Gatchel, R.J.; Liu, H. Whole-cortical graphical networks at wakeful rest in young and older adults revealed by functional near-infrared spectroscopy. *Neurophotonics* **2018**, *5*, 035004. https://doi.org/10.1117/1.NPh.5.3.035004.

33. Welch, P. The use of fast Fourier transform for the estimation of power spectra: a method based on time averaging over short, modified periodograms. *IEEE Transactions on audio and electroacoustics* **1967**, *15*, 70-73.
34. Xu, G.; Huo, C.; Yin, J.; Zhong, Y.; Sun, G.; Fan, Y.; Wang, D.; Li, Z. Test-retest reliability of fNIRS in resting-state cortical activity and brain network assessment in stroke patients. *Biomed. Opt. Express* **2023**, *14* 4217-4236.
35. Pruitt, T.; Wang, X.; Wu, A.; Kallioniemi, E.; Husain, M.M.; Liu, H. Transcranial Photobiomodulation (tPBM) With 1,064-nm Laser to Improve Cerebral Metabolism of the Human Brain In Vivo. *Lasers Surg Med* **2020**, *52*, 807-813. https://doi.org/10.1002/lsm.23232.
36. Truong, N.C.D.; Shahdadian, S.; Kang, S.; Wang, X.; Liu, H. Influence of the Signal-To-Noise Ratio on Variance of Chromophore Concentration Quantification in Broadband Near-Infrared Spectroscopy. *Frontiers in Photonics* **2022**, *3*, 908931. https://doi.org/10.3389/fphot.2022.90893.
37. Kolyva, C.; Tachtsidis, I.; Ghosh, A.; Moroz, T.; Cooper, C.E.; Smith, M.; Elwell, C.E. Systematic investigation of changes in oxidized cerebral cytochrome c oxidase concentration during frontal lobe activation in healthy adults. *Biomed Opt Express* **2012**, *3*, 2550-2566. https://doi.org/10.1364/BOE.3.002550.
38. Bainbridge, A.; Tachtsidis, I.; Faulkner, S.D.; Price, D.; Zhu, T.; Baer, E.; Broad, K.D.; Thomas, D.L.; Cady, E.B.; Robertson, N.J.; et al. Brain mitochondrial oxidative metabolism during and after cerebral hypoxia-ischemia studied by simultaneous phosphorus magnetic-resonance and broadband near-infrared spectroscopy. *NeuroImage* **2014**, *102 Pt 1*, 173-183. https://doi.org/10.1016/j.neuroimage.2013.08.016.
39. Bale, G.; Mitra, S.; Meek, J.; Robertson, N.; Tachtsidis, I. A new broadband near-infrared spectroscopy system for in-vivo measurements of cerebral cytochrome-c-oxidase changes in neonatal brain injury. *Biomed Opt Express* **2014**, *5*, 3450-3466. https://doi.org/10.1364/BOE.5.003450.
40. Park, J.; Lindberg, C.R.; Vernon III, F.L. Multitaper spectral analysis of high-frequency seismograms. *Journal of Geophysical Research: Solid Earth* **1987**, *92*, 12675-12684.
41. Babadi, B.; Brown, E.N. A review of multitaper spectral analysis. *IEEE Transactions on Biomedical Engineering* **2014**, *61*, 1555-1564.
42. Popov, T.; Oostenveld, R.; Schoffelen, J.M. FieldTrip Made Easy: An Analysis Protocol for Group Analysis of the Auditory Steady State Brain Response in Time, Frequency, and Space. *Front Neurosci* **2018**, *12*, 711. https://doi.org/10.3389/fnins.2018.00711.
43. Oostenveld, R.; Fries, P.; Maris, E.; Schoffelen, J.-M. FieldTrip: open source software for advanced analysis of MEG, EEG, and invasive electrophysiological data. *Computational intelligence and neuroscience* **2011**, *2011*.
44. Bastos, A.M.; Schoffelen, J.M. A Tutorial Review of Functional Connectivity Analysis Methods and Their Interpretational Pitfalls. *Front Syst Neurosci* **2015**, *9*, 175. https://doi.org/10.3389/fnsys.2015.00175.
45. Percival, D.B.; Walden, A.T. *Spectral analysis for physical applications*; cambridge university press: 1993.